Use of ^{18}F-FDG PET to Predict Response to First-Line Tuberculostatics in HIV-Associated Tuberculosis

Mike Sathekge[1], Alex Maes[2,3], Mpho Kgomo[4], Anton Stoltz[5], and Christophe Van de Wiele[6]

[1]Department of Nuclear Medicine, University of Pretoria, Pretoria, South Africa; [2]Department of Nuclear Medicine, AZ Groeninge, Kortrijk, Belgium; [3]Department of Morphology and Medical Imaging, University Hospital Leuven, Leuven, Belgium; [4]Department of Internal Medicine, Louis Pasture Hospital, Pretoria, South Africa; [5]Department of Infectious Diseases, University of Pretoria, Pretoria, South Africa; and [6]Department of Nuclear Medicine, University Hospital Ghent, Ghent, Belgium

This prospective pilot study examined the relationship between the severity and extent of tuberculosis as assessed by ^{18}F-FDG PET at the time of diagnosis and response to treatment or treatment failure at 4 mo. **Methods:** Twenty-four consecutive HIV patients with newly diagnosed tuberculosis were prospectively included in the study after providing written informed consent. Seventeen patients had pulmonary tuberculosis, and 7 patients had extrapulmonary tuberculosis. All patients underwent whole-body ^{18}F-FDG PET; none were receiving tuberculostatics at the time of the PET investigation. After undergoing ^{18}F-FDG PET, the patients were given tuberculosis treatment (the classic triad: isoniazid, rifampicin, and ethambutol) and reevaluated for treatment response: monthly assessment of sputum, smears, and cultures in patients who proved positive at the time of diagnosis, and clinical and radiologic (when relevant) assessment 4 mo after treatment instigation in all patients. Quantitative ^{18}F-FDG PET results (averaged ^{18}F-FDG maximum standardized uptake value [SUVmax] derived from early and delayed imaging), percentage change in SUVmax, and number of involved lymph node bastions were related to treatment response or failure. **Results:** Age, sex, viral load, CD4 status, duration of HIV treatment, SUVmax of lung and splenic lesions (early and delayed), and percentage change in SUVmax of lymph nodes were not significantly different between responders and nonresponders ($P \geq 0.3$). In contrast, SUVmax of involved lymph node bastions (both early and delayed) and number of involved lymph node bastions were significantly higher in nonresponders than in responders (respective P values were 0.03, 0.04, and 0.002). Using a cutoff of 5 or more involved lymph node bastions, responders could be separated from nonresponders with a sensitivity, specificity, and positive and negative predictive value of, respectively, 88%, 81%, 70%, and 93%. Using a cutoff of 8.15 for early SUVmax of lymph node bastions and of 10 for late SUVmax of lymph node bastions, a comparable sensitivity of 88% came at the cost of a lower specificity: 73% and 67%, respectively. **Conclusion:** In this pilot study, a cutoff of 5 or more involved lymph node bastions allowed for separation of tuberculostatic responsive and nonresponsive tuberculosis-infected HIV patients with a sensitivity of 88%, a specificity of 81%, and a negative predictive value of 93%. These findings warrant confirmation by additional studies on larger cohorts of patients.

Key Words: TBC; MDR; FDG PET; HIV

Because of deficiencies in knowledge of tuberculosis, as well as in the practices, programs, and strategies used to combat the disease and coinfection with HIV, the spread of multidrug-resistant (MDR) tuberculosis (tuberculosis that is resistant to at least isoniazid and rifampin) is posing a major health problem (*1,2*). In 2008, the number of MDR tuberculosis cases reached an estimated 390,000–510,000 (3.6% of all incident tuberculosis cases), and at least 150,000 deaths occur as a result of MDR tuberculosis each year (*3*).

Early detection of drug resistance in tuberculosis allows the initiation of an appropriate treatment, which may significantly affect the control of the disease: currently, more than two thirds of patients with MDR tuberculosis die. Both genotypic and phenotypic methods allowing assessment of MDR tuberculosis on tuberculosis bacilli isolated from fluids of infected patients are currently available (*4,5*). However, many of these tests are lengthy, taking from 6 to 16 wk before a diagnosis is obtained, and require infected body fluids such as sputum, urine, blood, or pleural fluid, which are not available or are nondiagnostic in up to 30% of tuberculosis-infected HIV patients. Up to 20% of patients presenting with pulmonary tuberculosis are culture-negative, and in most patients presenting with extrapulmonary tuberculosis, fluids for diagnostic analysis are unavailable (*5–8*).

In this prospective pilot study, the relationship between the severity and extent of tuberculosis as assessed by ^{18}F-FDG PET at the time of diagnosis and response to treatment or treatment failure at 4 mo was studied in HIV patients with newly diagnosed tuberculosis. Because all patients strictly adhered to the treatment regimen initiated and had no diseases or medications known to interfere with absorption of

tuberculostatics, treatment failure was considered a surrogate marker for MDR in those patients in whom body fluids were not available (clinical MDR).

MATERIALS AND METHODS

Approval for this study was granted by the Ethics Committee of the University Hospital of Pretoria.

Twenty-four consecutive HIV patients either with tuberculosis as proven by histology or a sputum smear or presenting with a high clinical suspicion of tuberculosis were prospectively included in the study after providing written informed consent. Seventeen patients had pulmonary tuberculosis, and 7 patients had extrapulmonary tuberculosis. Diagnosis of active tuberculosis was established by sputum microscopy and cultures in 8 patients, by histologic analysis of resected lymph nodes after ^{18}F-FDG PET (12 patients), or on a clinical basis (4 patients; long-term follow-up of minimally 6 mo with a favorable response to conventional tuberculostatics). Criteria for clinical diagnosis were based either on CT findings suggestive of pulmonary tuberculosis (branching linear structures, satellite nodules, or a well-defined nodule with central calcification) that improved with antituberculostatics or on a combination of clinical aspects (prolonged cough lasting more than 3 wk, chest pain and hemoptysis, low-grade remittent fever, chills, night sweating, appetite or weight loss, easy fatigability, lymph node swelling, and pleurisy) that responded favorably to tuberculostatics.

All patients underwent whole-body ^{18}F-FDG PET; none were on tuberculostatics at the time of the PET investigation. After undergoing ^{18}F-FDG PET, the patients began receiving tuberculosis treatment (the classic triad: isoniazid, rifampicin, and ethambutol) and were evaluated for treatment response: monthly assessment of sputum, smears, and cultures in those patients who proved positive at the time of diagnosis, and clinical and radiologic (when relevant) assessment 4 mo after treatment instigation in all patients. Response or nonresponse was determined using the Centers for Disease Control and Prevention guidelines on tuberculosis treatment (9). Quantitative ^{18}F-FDG PET results (averaged ^{18}F-FDG maximum standardized uptake value [SUVmax] derived from early and delayed imaging, percentage change in SUVmax, and number of involved lymph node bastions) were related to treatment outcome (response or failure).

Dual-Phase ^{18}F-FDG PET/CT

Whole-body ^{18}F-FDG PET scans were acquired on a dedicated PET/CT scanner (Biograph; Siemens) from the top of the skull to the pelvis. Patients were required to have fasted for a minimum of 4 h before ^{18}F-FDG injection. Blood glycemia was monitored with a portable capillary glucometer. Patients received a dose of ^{18}F-FDG based on their body weight using the following formula: ([body weight/10] + 1) × 37 MBq. PET/CT was performed 45 and 120 min after injection of ^{18}F-FDG. The acquisition duration per bed position was 3 min; 9 bed positions were used.

Images were acquired in 3-dimensional mode and reconstructed with and without attenuation correction (CT-based) using ordered-subset expectation maximization yielding axial, sagittal, and coronal slices. The ^{18}F-FDG PET images were analyzed for the presence or absence of sites of active or inactive tuberculosis by 2 experienced nuclear medicine specialists who were unaware of the clinical data and the results of morphologic imaging. Disagreements were resolved by consensus.

For diagnostic CT, the following parameters were used: collimation of 24 × 1.2 mm; gantry rotation time of 500 ms; tube voltage of 120 kV; effective tube current of 100 mAs with online tube current modulation, and table feed of 18 mm/rotation. Contrast enhancement was achieved by intravenous administration of 100 mL of nonionic contrast material (Ultravist; Bayer HealthCare Pharmaceuticals) at a rate of 2 mL/s. The matrix size was 512 × 512. CT contrast-enhanced images were analyzed for the presence or absence of sites of active or inactive tuberculosis by 2 experienced radiologists who were unaware of the clinical diagnosis or ^{18}F-FDG PET findings. Disagreements were resolved by consensus. The CT criteria for joint infection included the presence of joint effusion, juxtaarticular osteoporosis, joint space narrowing, indistinct cortical margins, marginal erosions, and sclerotic reaction. The CT criteria for osteomyelitis included early soft-tissue edema, an early periosteal reaction, and the presence of focal erosions.

Quantitative Analysis

Manually defined regions of interest on the attenuation-corrected early and delayed axial images were used to obtain SUVmax for all identified lesions. When the CT findings were positive, the corresponding CT image was used as an anatomic landmark. The regions that were considered included the cervical, hilar, mediastinal, axillary, portal-hepatic, paraaortic, pelvic, and inguinal regions. The number of sites (lymph node basins) of lymph node involvement was counted. When there were several lymph nodes in 1 basin, values were averaged. Percentage change in SUVmax from early to delayed images was calculated using the following formula:

$$\%DSUVmax = (SUV maxD - SUVmaxE)/SUVmaxE \times 100,$$

where D = delayed and E = early. In the presence of more than 1 basin or lung lesion, the SUVmax of lymph node bastions and the SUV max of lung lesions were averaged for statistical analysis.

Statistical Analysis

Statistical analysis was performed using SPSS version 15.0. The Fisher exact test was used to assess differences in sex between responders and nonresponders (clinical–MDR). The Kolmogorov–Smirnov test was used to assess the normalcy of the data. Differences in SUVmax (early or delayed), percentage change in SUVmax, and number of involved lymph node bastions between non-MDR and MDR patients were assessed using an unpaired nonparametric Wilcoxon test. Correlation analysis was performed using a Spearman rank test. P values less than 0.05 were deemed significant; tests were 2-tailed. Sensitivity, specificity, and positive and negative predictive values for differentiating non-MDR from MDR tuberculosis were calculated using the classic formulas. Receiver-operating-characteristic curve analysis was also performed.

RESULTS

The mean age of the whole patient group was 39 y (range, 25–64 y). There were 14 men and 10 women. Patient characteristics and results are shown in Table 1. All patients strictly adhered to their treatment regimen. None had a disease, or was taking a drug, known to inter-

TABLE 1
Patient Characteristics and Results

Patient no.	Sex	Age (y)	Viral load	CD4	HAART	LN no.	SUV LN 1	SUV LN 2	ΔSUV LN	LU no.	SUV LU 1	SUV LU 2	ΔSUV LU	Response to therapy	CRP
1	M	28	50	479	12	8	8.6	10.8	26	2	2.9	5.2	79	NR	206
2	F	25	643,211	105	0	3	4.8	7.1	48	1	5.6	9.9	75	R	67
3	M	47	189,000	237	3	1	2.4	2.5	4	2	3.1	3.7	19	R	32
4	M	36	50	459	24	7	11.8	19.6	66	—	—	—	—	NR	189
5	M	42	8,028	256	6	5	6.3	8.6	37	2	4.4	9.3	110	R	29
6	F	34	623	352	12	3	4.9	6.5	33	—	—	—	—	R	45
7	F	38	5,121	119	6	2	7.7	11.9	55	—	—	—	—	R	37
8	F	46	431	456	12	6	13.5	20.6	53	—	—	—	—	NR	162
9	F	34	50	524	24	3	6.9	10	45	1	7.8	13.5	73	R	103
10	M	43	345,216	53	0	4	9.2	16	74	1	7.8	9.3	19	R	177
11	F	27	753	109	3	1	17.2	21	22	2	13.2	18.1	37	R	142
12	M	45	188	476	9	1	9.7	15.4	49	1	7.1	9.8	38	R	75
13	M	43	20,345	277	6	7	10.2	15.2	49	2	12.8	19.7	53	NR	153
14	F	64	223,458	117	0	0	—	—	—	2	14.8	19.8	32	R	78
15	M	35	532,175	56	0	7	8.9	12.5	40	—	—	—	—	NR	98
16	M	53	50	489	20	1	5.4	5.2	16	2	6.4	8.4	30	R	121
17	F	26	763	199	4	5	13.8	16.4	19	2	4.7	5.8	23	NR	173
18	M	51	50	502	12	7	9	12.7	41	—	—	—	—	R	20
19	M	38	2,033	426	14	1	4.7	4.3	−9	2	3.6	4.4	22	R	33
20	F	35	569,000	59	0	6	11.8	16	36	1	10.2	16.4	61	NR	156
21	F	37	231,452	87	1	3	4.8	7.4	54	1	8.2	11.2	37	R	31
22	M	37	154,234	132	6	7	6.1	7.4	21	1	8.5	9.7	14	R	101
23	M	45	745	187	9	3	4.6	4.9	6	1	6.9	7.3	6	NR	48
24	M	32	960	189	24	1	3.2	3.3	3	0	—	—	—	R	16

Viral load = number of virus copy numbers/mL; CD4 = CD4 cell count/mL; LN no. = number of involved lymph node bastions; SUV LN 1 = average lymph node SUVmax on early images; SUV LN 2 = average lymph node SUVmax on delayed images; ΔSUV LN = percentage change over time in SUVmax of lymph nodes; LU no. = number of sites of lung involvement; SUV LU 1 = (average) lung lesion SUVmax on early images; SUV LU 2 = (average) lung lesion SUVmax on delayed images; ΔSUV LU = percentage change over time in SUVmax of lung lesions; CRP = C-reactive protein in mg/mL; NR = nonresponder; R = responder.

fere with tuberculostatic absorption. At follow-up (4 mo after tuberculosis treatment initiation), 8 patients were found not to have responded to the treatment, whereas the remaining 16 had responded favorably.

Nonresponders

In the 8 patients (4 men and 4 women) who did not respond to the initiated tuberculosis treatment, median viral load, CD4 count, and duration of highly active antiretroviral therapy (HAART) were, respectively, 745 copy numbers/mL (range, 50–569,000), 238/μL (range, 56–479), and 7.5 mo (range, 0–24 mo). Median C-reactive protein level was 159 mg/dL (range, 48–206 mg/mL).

All 8 patients were positive for lymph node involvement on ^{18}F-FDG PET (median number of involved bastions, 6; range, 3–8). Median early, delayed, and percentage change in SUVmax of ^{18}F-FDG–positive lymph node bastions for this patient group were, respectively, 11 (4.6–13.8), 15.6 (4.9–20.6), and 38% (6%–66%). Delayed SUVmax of involved lymph node bastions was significantly higher than early SUVmax ($P = 0.01$).

Five of the 8 patients (62%) also presented with lung involvement. Median early, delayed, and percentage change in SUVmax of lung lesions for this patient group were, respectively, 6.9 (2.9–12.8), 7.3 (5.2–19.7), and 53% (6%–79%). Delayed SUVmax of tuberculosis lung lesions was significantly higher than early SUVmax ($P = 0.04$).

Five of the 8 patients presented with splenic involvement. Median early, delayed, and percentage change in SUVmax of splenic lesions for this patient group were, respectively, 7.2 (5.3–7.6), 8.9 (6.1–9.5), and 17% (10%–30%). Delayed SUVmax for splenic lesions showed a trend toward being significantly higher than early SUVmax ($P = 0.08$).

Responders

In the 16 patients (9 men and 7 women) who responded favorably to the initiated tuberculosis treatment, median viral load, CD4 count, and duration of HAART were, respectively, 3,577 copy numbers/mL (range, 50–643,211), 213/μL (range, 53–524), and 6 mo (range, 0–24 mo). Median C-reactive protein level was 56 mg/dL (range, 16–177 mg/mL).

Fifteen of the 16 patients (94%) were positive for lymph node involvement on ^{18}F-FDG PET (median number of involved bastions, 2; range, 0–7). Median early, delayed, and percentage change in SUVmax of ^{18}F-FDG–positive lymph node bastions for this patient group were, respectively, 6.1 (2.4–17.2), 7.4 (2.5–21.0), and 37% (–9%–74%). Delayed SUVmax of involved lymph node bastions was significantly higher than early SUVmax ($P = 0.003$).

Twelve of the 16 patients (75%) also presented with lung involvement. Median early, delayed, and percentage change in SUVmax of lung lesions for this patient group were, respectively, 7.5 (3.1–14.8), 9.8 (3.7–19.8), and 35% (14%–110%). Delayed SUVmax of tuberculosis lung lesions was significantly higher than early SUVmax ($P = 0.002$).

Four of the 16 patients (25%) presented with splenic involvement. Median early, delayed, and percentage change in SUVmax of splenic lesions for this patient group were, respectively, 5.5 (4.2–6.6), 6.7 (5.9–7.3), and 18% (5%–69%). Delayed SUVmax of splenic lesions showed a trend toward being significantly higher than early SUVmax ($P = 0.07$).

Finally, 3 patients (19%) presented with bone or joint involvement, and 1 patient (6%) with pleural involvement.

Differences Between Responders and Nonresponders

Age, sex (Fisher exact test), viral load, CD4 status, duration of HAART, SUVmax of lung and splenic lesions (early and delayed), and percentage change in SUVmax of lymph nodes proved not significantly different between responders and nonresponders ($P \geq 0.3$).

In contrast, SUVmax of involved lymph node bastions (both early and delayed), number of involved lymph node bastions, and C-reactive protein level were significantly higher in nonresponders than in responders (corresponding P values were, respectively, 0.03, 0.04, 0.002, and 0.003) (Fig. 1).

The spleen tended to be more significantly involved in nonresponders than in responders (Fisher test, $P = 0.07$).

For a cutoff of 5 or more involved lymph node bastions, responders could be separated from nonresponders with a sensitivity, specificity, and positive and negative predictive values of, respectively, 88%, 81%, 70%, and 93% (receiver-operating-characteristic analysis; area under the curve, 0.879).

For a cutoff of 8.15 for early SUVmax of lymph node bastions and of 10 for late SUVmax of lymph node bastions, a comparable sensitivity of 88% came at the cost of a lower specificity: 73% and 67%, respectively. For a cutoff of 75 mg/mL for C-reactive protein levels, a comparable sensitivity of 88% came at the cost of an even lower specificity: 50%.
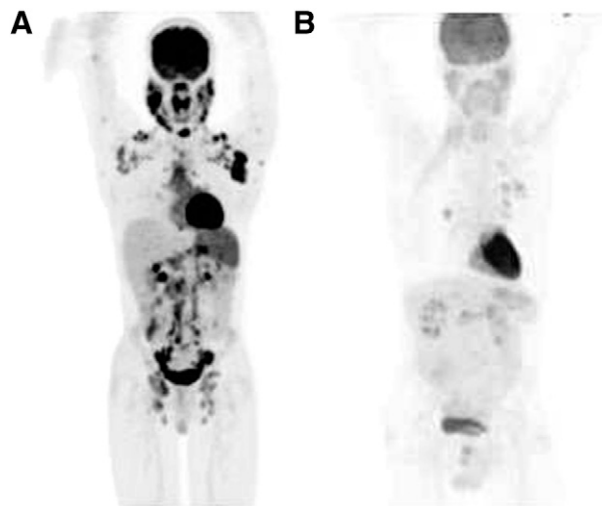
FIGURE 1. (A) ^{18}F-FDG PET image of patient 1, who failed to respond to therapy. Extensive involvement of 8 lymph node bastions is seen. (B) ^{18}F-FDG PET image of patient 12, who did respond favorably to therapy. Involvement of 1 lymph node basin (hilar) is seen, in addition to lung involvement.

DISCUSSION

This prospective pilot study studied the relationship between the severity and extent of tuberculosis—pulmonary and extrapulmonary—as assessed by ^{18}F-FDG PET at the time of diagnosis and response to treatment or treatment failure at 4 mo.

No difference in the SUVmax of sites of lung involvement was found between responder and nonresponder HIV-positive patients with clinical MDR tuberculosis. Hypothetically, this may relate to the plethora of variables and their interindividual contribution to ^{18}F-FDG uptake in tuberculosis granuloma (e.g., differences in tuberculosis strain virulence, expression levels of the Mal [MyD88 adaptor-like] protein TIRAP [Toll-interleukin 1 receptor domain–containing adaptor protein], and release of proinflammatory cytokines by giant cells and epitheloid macrophages), as well as to the variability in the level of immune suppression due to HIV in the patients studied (10–17). In the series presented, no significant differences were found in viral load or CD4 cell count between nonresponders and responders.

The involved lymph nodes proved metabolically significantly more active than the lymph nodes of HIV-alone or tuberculosis-alone patients (11,18,19). This finding most likely reflects the impact of the 2 diseases on each other: HIV impairs the host's ability to contain new tuberculosis infections (20,21), and tuberculosis may accelerate the clinical course of the HIV infection. Importantly, in the series presented, the number of involved lymph node bastions and the intensity of ^{18}F-FDG uptake by involved lymph nodes proved significantly higher in nonresponders to tuberculostatics than in responders. The lymph nodes play an essential role in mounting a defense to invading tuberculosis (22,23). At the site of tuberculosis invasion, immature dendritic cells internalize tuberculosis bacilli and then home to the nearest lymph node bastion, where they mature and migrate to the T-cell area to present tuberculosis antigens and recruit naïve T-cells. Those cells will differentiate into T-effector cells, which will help to eliminate or stabilize the tuberculosis infection. When confronted with an immunocompromised host and a particular virulent strain of bacteria, these defense mechanisms in the local lymph nodes may not be activated quickly enough to contain the initial wave of infection, with uncontrollable levels of bacteria spreading throughout the body, activating additional lymph nodes. Such dynamics could explain why ^{18}F-FDG PET found more bastions of lymph node involvement in nonresponders than in responders.

Splenic, pleural, and joint and bone involvement are less frequent manifestations of extrapulmonary tuberculosis: these 3 manifestations occurred only in responders (7). In contrast, splenic involvement tended to be more frequent and more pronounced in nonresponders than in responders. This finding warrants further exploration in larger series of patients.

Early detection of drug resistance in tuberculosis allows the initiation of an appropriate treatment, which may significantly affect patient survival (3). In an estimated 30% of tuberculosis-infected HIV patients, MDR status cannot be assessed using available laboratory methods (4–8). In addition, obtaining a diagnosis with these tests may take from 6 to 16 wk, a delay that, when the physician is confronted with an acute form of tuberculosis, may prove clinically unacceptable. In the study reported, the use of a cutoff of 5 for the number of involved lymph node bastions as assessed by ^{18}F-FDG PET allowed for the separation of nonresponders from responders with a sensitivity of 88%, a specificity of 81, and, importantly, a negative predictive value of 93%. When a cutoff of 8.15 for early SUVmax of lymph node bastions and 10 for late SUVmax of lymph node bastions was used, a comparable sensitivity of 88% came at the cost of a lower specificity: 73% and 67%, respectively. At a comparable sensitivity of 88%, C-reactive protein measurements yielded a specificity of only 50%. Given that all patients strictly adhered to the treatment regimen initiated and had no diseases or medications known to interfere with absorption of tuberculostatics, treatment failure in this patient population may be considered an acceptable surrogate for MDR (clinical MDR). Thus, our findings suggest that ^{18}F-FDG PET may indirectly assess MDR status in tuberculosis patients and that ^{18}F-FDG PET has potential to become a valuable clinical adjunct to the already available genotypic and phenotypic tests in patients for whom such tests are not feasible, are inconclusive, or are too lengthy to be of clinical relevance.

CONCLUSION

In this pilot study, a cutoff of 5 or more involved lymph node bastions allowed for separation of tuberculostatic responsive and nonresponsive tuberculosis-infected HIV patients with a sensitivity of 88%, a specificity of 81%, and a negative predictive value of 93%. These findings warrant confirmation by additional studies on larger cohorts of patients.

DISCLOSURE STATEMENT

REFERENCES

1. Caminero JA. Multidrug-resistant tuberculosis: epidemiology, risk factors and case findings. *Int J Tuberc Lung Dis.* 2010;14:382–390.
2. Migliori GB, D'Arcy Richardson M, Sotgiu G, Lange C. Multidrug-resistant and extensively drug-resistant tuberculosis in the West: Europe and United States—epidemiology, surveillance, and control. *Clin Chest Med.* 2009;30:637–665.
3. *Multidrug Resistant and Extensively Drug-Resistant TB (M/XDR-TB): 2010—Global Report on Surveillance and Response.* Geneva, Switzerland: WHO Press:1–71. WHO/HTM/TB/2010.3.
4. Van Deun A, Martin A, Palomino JC. Diagnosis of drug-resistant tuberculosis: reliability and rapidity of detection. *Int J Tuberc Lung Dis.* 2010;14:131–140.
5. Ahmad S, Mokaddas E. Recent advances in the diagnosis and treatment of multidrug-resistant tuberculosis. *Respir Med.* 2009;103:1777–1790.
6. Long R. Smear-negative pulmonary tuberculosis in industrialized countries. *Chest.* 2001;120:330–334.
7. Golden MP, Vikram HR. Extrapulmonary tuberculosis: an overview. *Am Fam Physician.* 2005;72:1761–1768.

8. Mendelson M. Diagnosing tuberculosis in HIV-infected patients: challenges and future prospects. *Br Med Bull.* 2007:81–82, 149–165.

9. Centers for Disease Control and Prevention. Treatment of tuberculosis: American Thoracic Society, CDC, and Infectious Disease Society of America. *Morb Mortal Wkly Rep.* 2003; 52:1–88.

10. Goo JM, Im JG, Do KH, et al. Pulmonary tuberculoma evaluated by means of FDG PET: findings in 10 cases. *Radiology.* 2000;216:117–121.

11. Sathekge M, Maes A, Kgomo M, Stoltz A, Pottel H, Van de Wiele C. Impact of FDG PET imaging on the management of TB treatment: a pilot study. *Nuklearmedizin.* 2010;49:35–40.

12. Bulut Y, Michelsen KS, Hayrapetian L, et al. Mycobacterium tuberculosis heat shock proteins use diverse Toll-like receptor pathways to activate pro-inflammatory signals. *J Biol Chem.* 2005;280:20961–20967.

13. Taype CA, Shamsuzzaman S, Accinelli RA, Espinoza JR, Shaw MA. Genetic susceptibility to different clinical forms of tuberculosis in the Peruvian population. *Infect Genet Evol.* 2010;10:495–504.

14. Jeong YJ, Lee KS. Pulmonary tuberculosis: up-to-date imaging and management. *AJR.* 2008;191:834–844.

15. Kubota R, Yamada S, Kubota K, Ishiwata KL, Tamahashi N, Ido T. Intratumoral distribution of fluorine-18-deoxyglucose in vivo: high accumulation in macrophages and granulation tissues studied by microautoradiography. *J Nucl Med.* 1992;33:1972–1980.

16. de Noronha AL, Báfica A, Noguiera L, Barral A, Barral-Netto M. Lung granulomas from mycobacterium tuberculosis/HIV-1 co-infected patients display decreased in situ TNF production. *Pathol Res Pract.* 2008;204:155–161.

17. Hirsch CS, Johnson JL, Okwera A, et al. Mechanisms of apoptosis of T-cells in human tuberculosis. *J Clin Immunol.* 2005;25:353–364.

18. Sathekge M, Maes A, Kgomo M, Van de Wiele C. FDG uptake by lymph nodes of HIV patients is inversely related to CD4 cell count. *Nucl Med Commun.* 2010;31:137–140.

19. Sathekge M, Goethals I, Maes A, Van de Wiele C. Positron emission tomography in patients suffering from HIV-1. *Eur J Nucl Med Mol Imaging.* 2009;36:1176–1184.

20. Wallis RS, Vjecha M, Amir Thamasseb M, et al. Influence of tuberculosis on human immunodeficiency virus (HIV-1): enhanced cytokine expression and elevated beta-2-microglobulin HIV-1 associated tuberculosis. *J Infect Dis.* 1993;167:43–48.

21. Lederman M, Georges D, Kusner D, et al. Mycobacterium tuberculosis and its purified protein derivative activate expression of the human immunodeficiency virus. *J Acquir Immune Defic Syndr.*1994;7:727–733.

22. Marino S, Kirschner DE. The human immune response to mycobacterium tuberculosis in lung and lymph node. *J Theor Biol.* 2004;227:463–486.

23. Dietrich J, Doherty TM. Interaction of mycobacterium tuberculosis with the host: consequences for vaccine development. *APMIS.* 2009;117:440–457.